Simulation and Dynamic Characteristics Research on Three-level Power Amplifier of AMB

Wentao Yu[1,a], hongwei Li [1,b], Yunpeng Zhang[1,c] , *Shuqin Liu [1,d]

[1]ShandongUniversity, Jingshi Road 17923, Jinan city, Shandong province, China
E-mail:[a] wintop@sdu.edu.cn [b] lhw08@sdu.edu.cn [c] zhangyp@sdu.edu.cn [d] lshuqin@sdu.edu.cn
* Tel.: +86-0531-81696186; fax: +86-0531-88399385. E-mail address: Lshuqin@sdu.edu.cn.

***Abstract* — Active Magnetic Bearing (AMB) with high-speed, long life, low power consumption and without lubrication system, it has been widely used. Power Amplifier is a core component of active magnetic bearing, determines the AMB performance directly. In this paper, based on the detailed analysis of the working principle of three-level power amplifier, the simulation model of power amplifier for AMB based on FPGA chip is built, which using MATLAB/Simulink Power System block and M-file. On this simulation platform, the influential factors of dynamic characteristics for three-level power amplifier, bus voltage, proportional coefficient and differential coefficient are analyzed. Experimental results show that the simulation systems and experimental results are in good agreement. So the method offers a new thought for analyzing the dynamic characteristics of the power amplifier for AMB.**

Keywords - Three-level, Power Amplifier, Dynamic characteristics, Matlab, AMB

I. INTRODUCTION

Active Magnetic Bearing (AMB) is a new type of non-contact bearing which use electromagnetic force controlled rotor suspension, compared with conventional bearings, it has many advantages, such as high-speed, no friction, long life, low power consumption and without lubrication, etc.[1], It is widely used in turbine machinery, centrifuges, high-speed machine tools, flywheel energy storage, vacuum and clean room technology, artificial heart pumps and spacecraft attitude control gyroscope and other fields.[2]-[5]

In the magnetic bearing control system, the role of the power amplifier is generated coil current according to the control system output signal, which generates the appropriate electromagnetic force to ensure the stability of the suspension of the rotor [5]. Therefore, as the execution unit of AMB control system, power amplifier has not only good linearity to ensure small current signal distortion, but also has sufficient bandwidth to ensure the active magnetic bearing system has good dynamic characteristics, suppress high-frequency vibration of the rotor. Depending on the generation principle, the power amplifier can be divided into linear power amplifier and switching power amplifier, since the switching power amplifier with low power consumption and high conversion efficiency advantages, has been applied in most AMB system. There are two kinds of commonly switching power amplifier, two-level and three-level. The current ripple of two-level switching amplifier is related with the DC bus voltage[6], if increasing the DC bus voltage in order to improve the dynamic characteristics of the AMB, it will increasing the coil current ripple at the same time. The current ripple of three-level Switching Power Amplifier is unaffected by the DC bus voltage and therefore more suitable for high-power active magnetic bearings. Three-level model is emerging control way in recent years, it adds a free-wheeling mode based on two-level power amplifier, which greatly reducing the current ripple.

At present, power amplifiers of AMB are analyzed as a first-order inertia delay loop, equivalent linear models of amplifier [6]-[9]. But in practice, the nature of switching power amplifier is non-linear, and the accuracy of switch power amplifier is not guaranteed if it is seen as first-order inertia equivalent amplifier. The circuit simulation software Multisim is used to build math modeling for switching power amplifier in reference [10]. This approach is limited by the software that comes with the model library, for some modules that is no in simulation modules can only approximate, with some limitations. Based on MATLAB/Simulink using power system block(PSB), the simulation model of the switching power amplifier is derived in order to analyze the system performance in reference[11], while this model While this model does not fit the switch power amplifier that the PWM signals generated by the FPGA chip or other digital processing chip(DSP), without considering the input saturation and time delay in AD sampling , time delay in program execution, the PID parameters and bus voltage are changed, which will affect the accuracy of simulation characteristic analyze of power amplifier. In reference [12] based on the analysis of three-level power amplifier principle, the nonlinear circuit model was replaced by using Fourier series and the transfer function of the nonlinear net was established, which obtain A closed-loop system math model of three-level power amplifier. It is only considers the general characteristics of the switching power amplifier, but the power amplifier control parameters based FPGA or DSP program of the switch for switching power amplifier not taken into account. Therefore, the simulation in this paper, in addition to use power system block (PSB) in MATLAB/Simulink to complete full bridge circuit and a current sampling circuit, but also uses M functions in MATLAB to simulate FPGA or DSP internal data processing, so that it can complete a more accurate characteristics of magnetic bearings digital amplifier emulation.

II. THE PRINCIPLE OF THREE-LEVEL POWER AMPLIFIER ANALYSIS

As shown in Fig.1 is a main circuit topology of three-level full-bridge power amplifier, which is made of four MOSFFET, the electromagnetic coil in the middle of circuit is represented by an equivalent inductance L and an equivalent resistance R. Full-bridge circuit can generate bi-directional current, which can be used in active magnetic bearing, also can be used in electromagnetic and permanent magnet hybrid bearing.

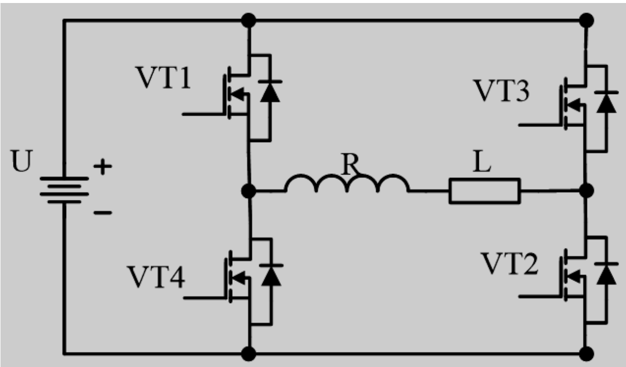

Fig.1 The main circuit topology of three-level power amplifier

To illustrate the three-level principles, the switching function Si was introduced.

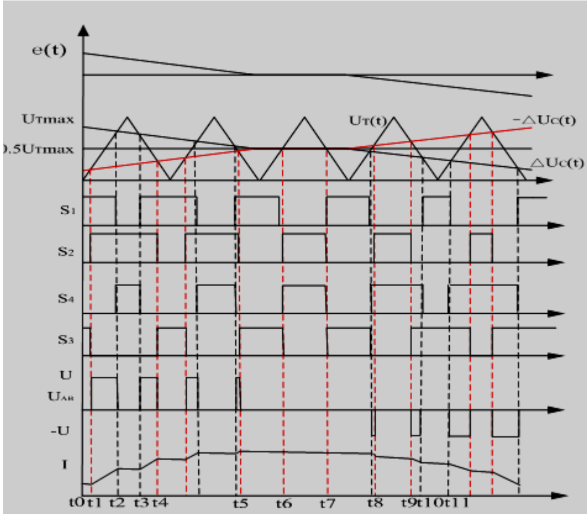

Fig.2 three-level PWM pulse generator schematic

$$S_i = \begin{cases} 1, & \text{when } VT_i \text{ on} \\ 0, & \text{when } VT_i \text{ off} \end{cases} \quad (1)$$

For the full-bridge circuit, the MOSFFETs (VT1 ~ VT4) are control respectively, the control signals of each side arm power tube are complement. Each power tube switching functions satisfy:

$$S_1 = \begin{cases} 1, & \text{when } 0.5U_{T\max} + e(t) < U_T(t) \\ 0, & \text{when } 0.5U_{T\max} + e(t) > U_T(t) \end{cases} \quad (2)$$

$$S_2 = \begin{cases} 1, & \text{when } 0.5U_{T\max} - e(t) > U_T(t) \\ 0, & \text{when } 0.5U_{T\max} - e(t) < U_T(t) \end{cases} \quad (3)$$

$$S_3 = 1 - S_2 \quad (4)$$

$$S_4 = 1 - S_1 \quad (5)$$

where: $U_{T\max}$ is the maximum value of the triangular carrier signal;

e(t) is the error between the input control signal and coil current $e(t) = Uc - U_L$;

$U_T(t)$ is the triangular carrier signal;

Fig. 2 shows a schematic of three-level PWM pulse generator, e(t) is the error signal, U_{AB} is voltage applied across the coil, I is the coil current. According to the error signal e(t), it can be divided into three statuses: the coil current charging, the coil current freewheeling and the coil current discharge.

DOI 10.5013/IJSSST.a.17.29.09 ISSN: 1473-804x online, 1473-8031 print

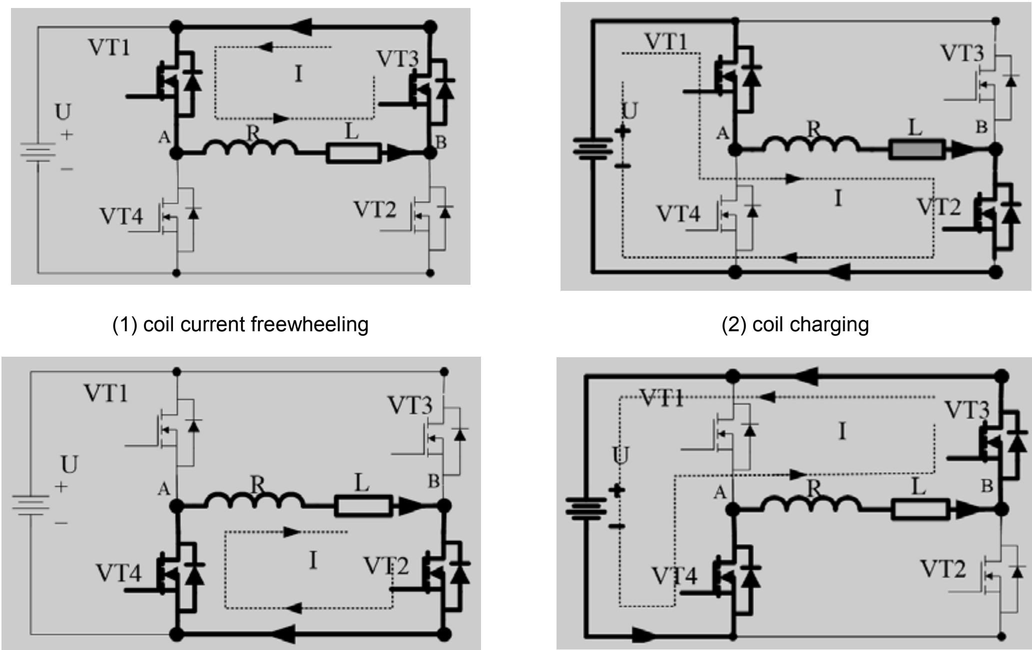

(1) coil current freewheeling

(2) coil charging

(3) coil current freewheeling

(4) coil discharge

Fig.3 three-level PWM current direction of the state diagram

A. Coil Current Charging

As shown in t_0-t_5 time in Fig. 2，when the error signal e(t) is greater than zero, the duty cycle of the switching function s1 and s2 are more than 50%, And proportional to the value of e(t), the coil current in freewheeling mode and charging mode. When Time is t_0-t_1, the VT1 and VT3 are turn on, the coil current is freewheeling, shown in Fig. 3(1). When Time is t_1-t_2, the MOSFFETs VT1 and VT2 are turn on, the coil current is charging, shown in Fig. 3(2). When Time is t_2-t_3, the VT2 and VT4 are turn on, the coil current is freewheeling, shown in Fig. 3(3).

When the coil current is in the freewheeling state, as shown Fig. 3 (1) and 3 (3), the current changes can be obtained by solving differential equations at the time [t_0-t_1]:

$$i_1 = i_0 - \frac{iR_{ON}}{R}\left(1 - e^{-\frac{R}{L}(T_1 - T_0)}\right) \tag{6}$$

Where: i_1 is the coil current at the t_1;

i_0 is the coil current at the t_0;

i is the average coil current;

R_{ON} is the total resistance when the power MOSFET is turn on;

R is the coil equivalent resistance;

L is the coil equivalent inductance;

T_0 is the start time for the freewheeling state;

T_1 is the end time for the freewheeling state;

Due to the high switching frequency, T_1-T_0 << 1， The equation (6) can be simplified into:

$$i_1 = i_0 - \frac{iR_{ON}}{L}(T_1 - T_0) \tag{7}$$

Since the Ron is small, so you can approximate that $i_1 \approx i_0$.

When the coil current is in the charging state, as shown Fig. 3 (2), the current changes can be obtained by solving differential equations at the time [t_2-t_3]:

$$i_3 = i_2 + \frac{U_{AB} - iR_{ON}}{R}\left(1 - e^{-\frac{R}{L}(T_3 - T_2)}\right) \tag{8}$$

Where: i_2 is the coil current at the t_2 time;

i_3 is the coil current at the t_3 time;

T_2 is the start time for the charging state;

T_3 is the end time for the charging state;

Due to the high switching frequency, T_3-T_2 << 1， The equation (8) can be simplified into:

$$i_3 = i_2 + \frac{U_{AB} - iR_{ON}}{L}(T_3 - T_2) \tag{9}$$

While it contains two states: coil current charging and coil current freewheeling, but current change is small in the coil current freewheeling. Throughout the time t0-t5, the coil

DOI 10.5013/IJSSST.a.17.29.09

ISSN: 1473-804x online, 1473-8031 print

current overall is increased.

B. Coil Current Freewheeling

As shown time t_5-t_7 in Fig. 2, when error signal e(t) is zero, the duty cycle of the switching function s1 and s2 are 50%, the coil current is in freewheeling mode and the value is unchanged basically. When Time is t_5-t_6, the VT1 and VT3 are turn on, the coil current is freewheeling, shown in Fig. 3(1). When Time is t_6-t_7, the VT2 and VT4 are turn on; the coil current is freewheeling, shown in Fig. 3(3). The equation of the coil current voltage change is equation (6) and equation (7).

C. Coil Current Discharging

As shown in t_8-t_{11} time in Fig. 2， when the error signal e(t) is less than zero, the duty cycle of the switching function s1 and s2 are less than 50%, And inversely proportional to the value of e(t) , the coil current is in freewheeling state and discharging mode. When Time is t_8-t_9, the VT2 and VT4 are turn on, the coil current is freewheeling, shown in Fig. 3(3). When Time is t_9-t_{10}, the MOSFFETs VT3 and VT4 are turn on; the coil current is discharging, shown in Fig. 3(4). When Time is t_{10}-t_{11}, the VT1 and VT3 are turn on, the coil current is freewheeling, shown in Fig. 3(1).

When the coil current is in the discharging state, as shown Fig. 3 (4), the current changes can be obtained by solving differential equations at the time [t10-t11]:

$$i_{11} = i_{10} - \frac{U_{AB} + iR_{ON}}{R}\left(1 - e^{-\frac{R}{L}(T_{11} - T_{10})}\right) \quad (10)$$

Due to the high switching frequency, T_{11}-T_{10} << 1，The equation (8) can be simplified into:

$$i_{11} = i_{10} - \frac{U_{AB} + iR_{ON}}{L}(T_{11} - T_{10}) \quad (11)$$

According to the equation (6) - (11)，for the same load, the change of coil current is only relation with this moment bus voltage, because the UAB >> $iR_{ON,}$ so the amount of current change in freewheeling mode is much less than the current change in charging and discharge mode, so the coil current ripple of three-level power amplifier is very small. According to the literature [5], the current ripple of three level power amplifiers is:

$$\Delta i = \frac{U_{VD} + U_{ON} + U_R}{2fL} \quad (12)$$

where:

Δi is the coil current ripple

U_{VD} is the voltage drop of the freewheeling diode

U_{ON} is the voltage drop of the switching MOSFET

U_R is the voltage drop of the coil equivalent resistance

f is the power amplifier switching frequency

L is the equivalent inductance of coil

Equation (12) is a current ripple of half-bridge circuit three level power amplifier, but the conclusion is basically the same with full-bridge circuit. It can be seen that the coil current ripple does matter with bus voltage U, and the others voltage drop are very small compared with bus voltage, so in order to improve the dynamic response of the amplifier to improve bus voltage, it won’t increasing the coil current ripple.

III.THE ESTABLISHMENT OF THREE-LEVEL AMPLIFIER SIMULATION MODELS

A. Induction of the three-level power amplifier based on FPGA

Fig. 4 is a three-level power amplifier circuit schematic, it is mainly composed of the following components: AD circuit, PWM generating circuit, isolation and driver amplifier circuit, the full-bridge circuit, the electromagnetic coil and a current sensor. The input control signals and the current feedback signals are converted into a digital signal by AD circuit and output to the PWM generate circuit; the generated PWM signals are amplified by isolation and driver amplifier circuit, at last to produce the required current of magnetic bearings coil by full bridge.

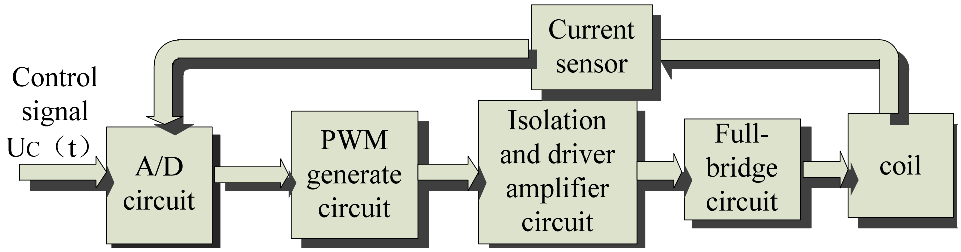

Fig. 4 Schematic of three-level power amplifier

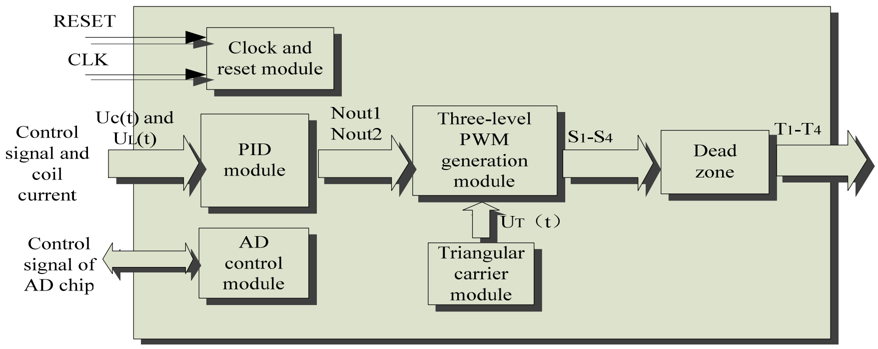

Fig.5 FPGA functional block diagram

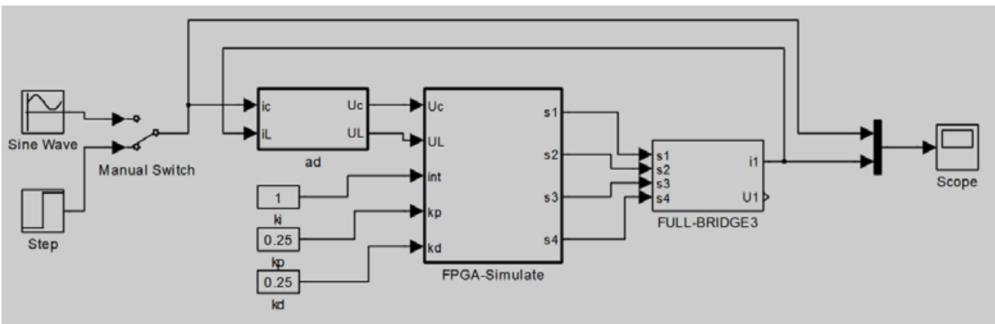

Fig.6 Overall system model diagram of simulation of power amplifier

PWM generation circuit is the core part of the power amplifier; its function is performed by FPGA chip. As Fig. 5 shown, the function module in FGPA includes AD control module, PID module, three-level PWM generation module, the dead zone, the triangular carrier generator module. the function of AD control module is control the AD chip to convert the analog signal to digital signal, PID module generate the PWM duty cycle N_{out1} and N_{out2} corresponding coils according to the error signal between the control signal Uc(t) and the current signal U_L(t). Three-level PWM generator module generate four PWM signals S1-S4 of full-bridge circuit according to the duty cycle N_{out1} and N_{out2}, the triangular carrier signal is provided by the triangular carrier module. The PWM signals S1-S4 are inputted to dead zone module to add dead time to prevent one side arm of full-bridge circuit are turned on at the same time.

B. Establish simulation model

Three-level power amplifier simulation model of AMB is built in Simulink environment of the MATLAB environment, Overall system model diagram shown in Fig. 6. According to the modular principle, the system is divided into three functionally independent modules, AD sampling module, FPGA-simulation module and a full-bridge circuit module.

Fig.7 is AD sampling block diagram, which is compose of the proportional link, the delay link and saturation limit link, the proportional link simulates the process which convert analog into digital, the proportion value is relate with the conversion accuracy and input voltage ranged of AD chip. In this paper, the AD chip is MAX125, the input voltage range is ±5V, and he digital conversion accuracy is 14 bits, so the proportion value is 1638. The delay link simulates the sampling period of AD chip, the value is 50μs. The saturation limit link simulates the conversion accuracy of AD chip, the value is 16383.

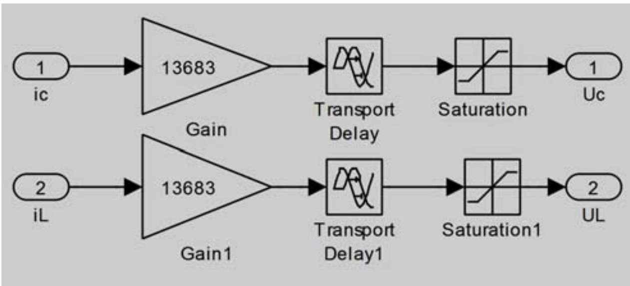

Fig.7 AD sampling block diagram

FPGA simulation module is completely in accordance with the procedures of internal FPGA signal processing, with the M files in each module for information processing.

Fig. 8 is a simulation block diagram of FPGA internal processing, control signals Uc and coil current signals U_L are input, the triangular carrier frequency is provided by Counter Limited module of the Matlab. For the PID_control module, the control signal U_{L1} and coil current signal U_{C1} are calculated according to equation (13) to (15) and the PWM duty cycle count value Nout1 and Nout2 of full-bridge circuit are obtained.

$$N_{out1} = 0.5U_{T\max} + \left[(K_p \times e + K_i \times e_i + K_d(e+e_p)\right] \quad (13)$$

$$N_{out2} = 0.5U_{T\max} - \left[K_p \times e + K_i \times e_i + K_d(e-e_p)\right] \quad (14)$$

$$e = U_{C1} - U_{L1} \quad (15)$$

Where $U_{T\max}$: is maximal value of triangular carrier signal

K_p : is proportionality coefficient

K_i : is integration coefficient

K_d : is differential coefficient

e: is error current time

e_i : is the sum of all previous errors

e_p : is the last error

U_{C1} : is the control signal of the upper coil of AMB

U_{L1} : is the coil current of the upper coil of AMB

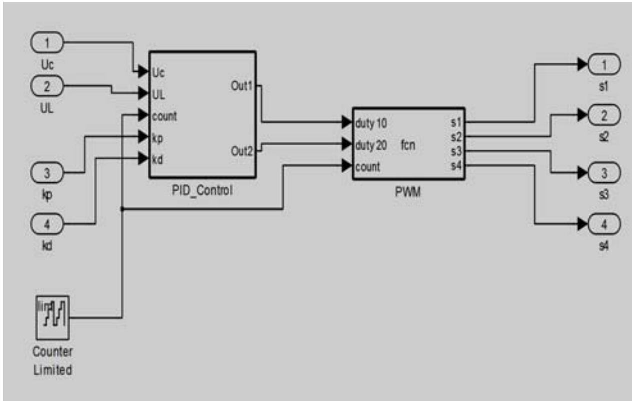

Fig.8 a simulation block diagram of FPGA internal processing

The value N_{Out1} and N_{Out2} are calculated to the PWM signals of full-bridge according to equation (2) - (5) by PWM generation module, PID_control module and PWM generation module are embedded function module which written by M files. Because the PID_control module need to use the previous data, the unit delay module 1 / Z is used, as shown in Fig. 9.

Full-bridge circuit is used SIMPowerSystems library element in MATLAB to simulate, as shown in Fig. 10. The switching power tubes used the MOSFET modules of SIMPowerSystems library, the connection according to the full bridge circuit.

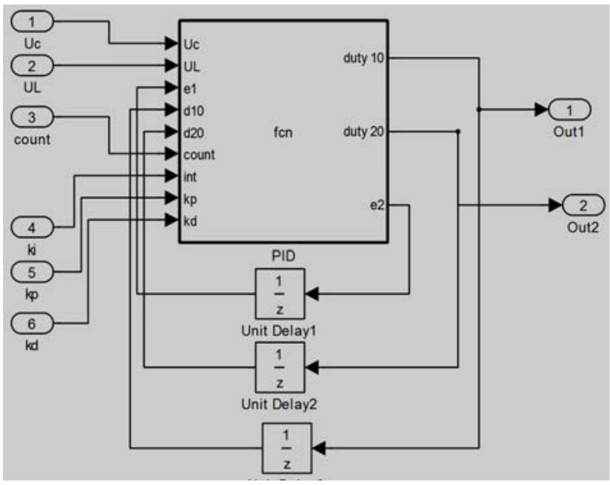

Fig.9 PID_control module

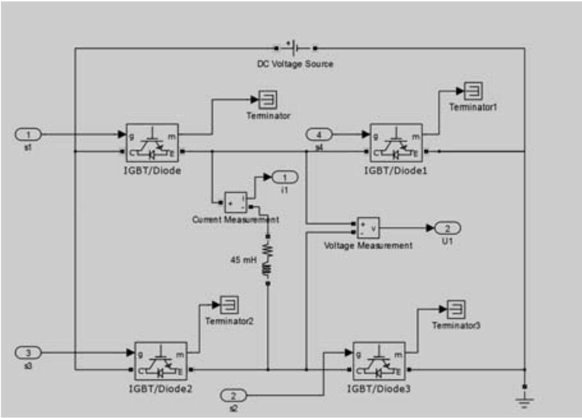

Fig.10 the full-bridge module

IV.THE SIMULATION OF POWER AMPLIFIER DYNAMIC FEATURE AND EXPERMENTAL VERIFICATION

The established simulation module of three-level power amplifier is test at different parameters with step signal input, the results is obtained and analyzed the effect of different parameters of the three-level amplifier, Simulation results are compared with the actual test results, verify the accuracy of the simulation results. The main parameters of the simulation experiments as shown in Table I.

TABLE I. THE SIMULATE PARAMETERS OF THREE-LEVEL POWER AMPLIFIER

Parameter	value
Equivalent inductance（L）	15mH
Equivalent resistance（R）	1Ω
Triangular carrier frequency（f）	20KHz
The on-resistance of MOSFET (IRF460)	0.27Ω
The gain factor of current sensor	1V/A

A. Simulation of the dynamic response at difference bus voltage

Frist test is the tracking speed of coil current when the bus voltage is difference, its bus voltages are 80V, 120V and 160V. PID parameters of simulation modules are: Kp=0.5; Kd=0.5; Ki=1; Fig. 11 (1) is the simulation results at different bus voltages; Fig. 11 (2) is the test results at 80 V, Fig. 11 (3) is the test results at 120 V , Fig. 11 (4) is the test results at 160 V . From Fig. 11 it can be concluded that the simulation results more consistent with the actual test result, the rising time of coil current speed is 0.96ms at 80V, 0.48ms at 120V and 0.24ms at 160V. As the bus voltage increases, the responses speed of coil current faster. The response speed of coil current hysteresis step signal is about 0.3ms, which is due to the delay time of signal transmission and other AD sampling chip delay.

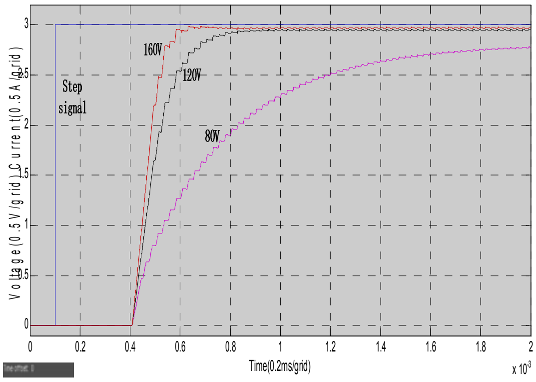

(1) The simulation results at different bus voltages

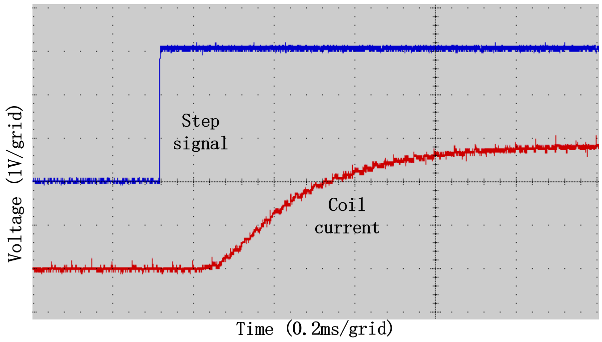

(2) The test results at 80V

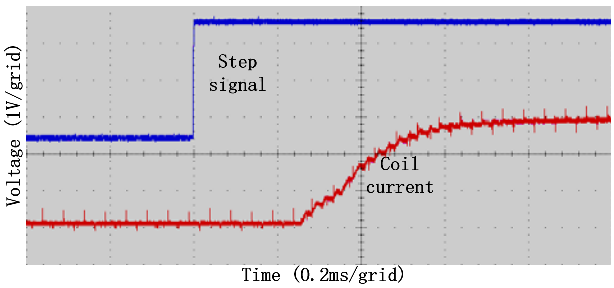

(

3) The test results at 120V

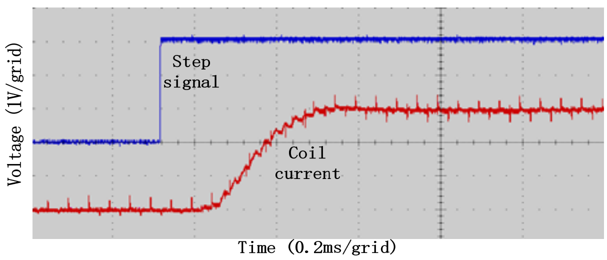

(4) The test results at 160V

Fig.11 the comparison of simulation results and test results at different voltages

B. Simulation of the dynamic response with different Kp

Fig. 12 is the Simulation and actual test result of the dynamic response at the same voltage for different Kp; The bus voltage is 120, control parameters are Ki =1; Kd=0.5; With Kp increases, the response speed of the coil current is increased, but the impact is smaller than the bus voltage, if more than a certain range, the overshoot becomes large.

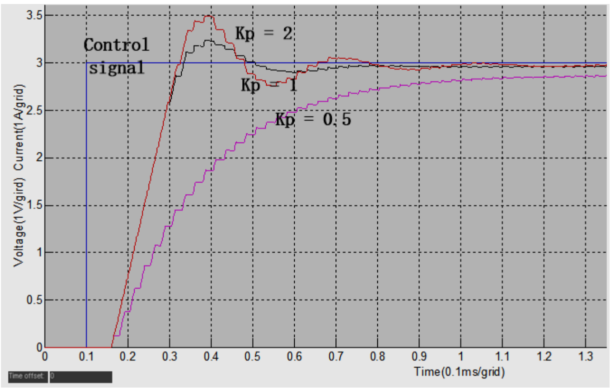

(1) The simulation results at different bus voltages

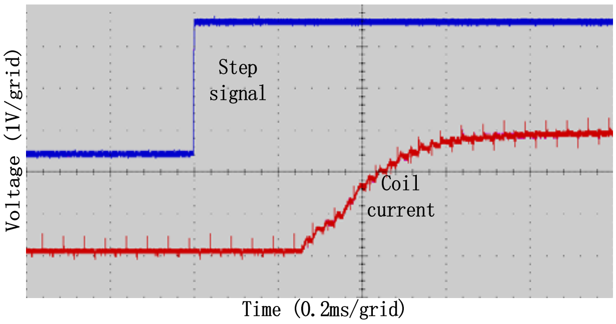

(2) The test result with Kp =0.5

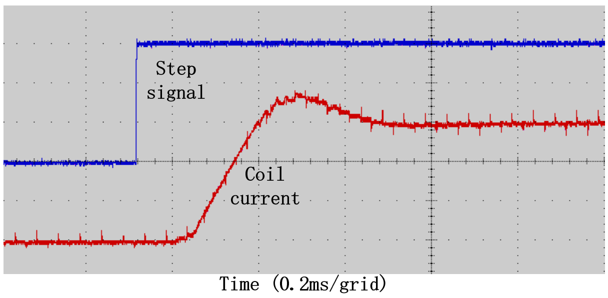

(3) The test result with Kp =1

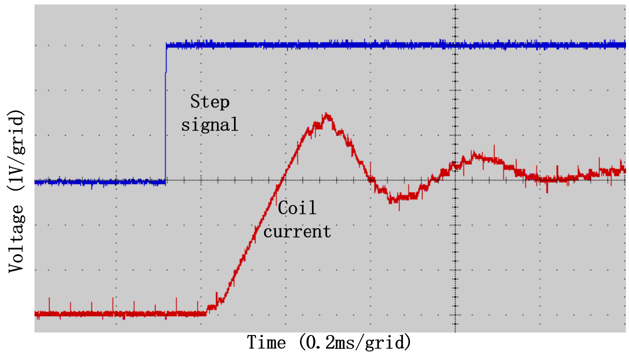

(4) The test result with Kp =0.5

Fig. 12 the comparison of simulation results and test results with different Kp

C. Simulation of the dynamic response with different Kd

Fig. 13 is the Simulation and actual test result of the dynamic response at the same voltage for different Kd; The bus voltage is 120, control parameters are Kp =1; Ki=1; With Kp increases, the response speed of the coil current is increased, but the impact is smaller than the bus voltage and **kp.**

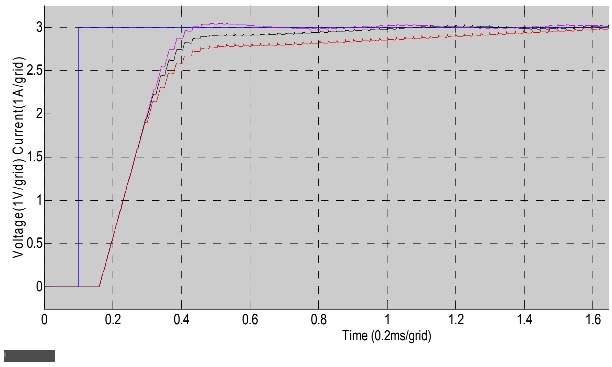

(1) The simulation results at different bus voltages

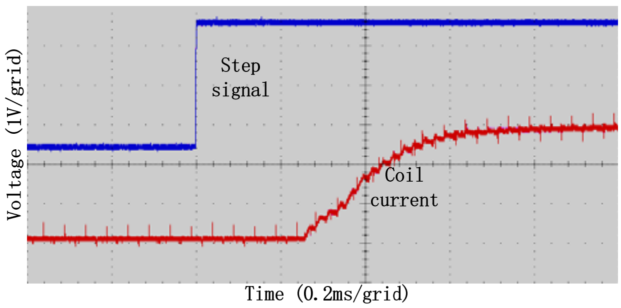

(2) The test result with Kd =1

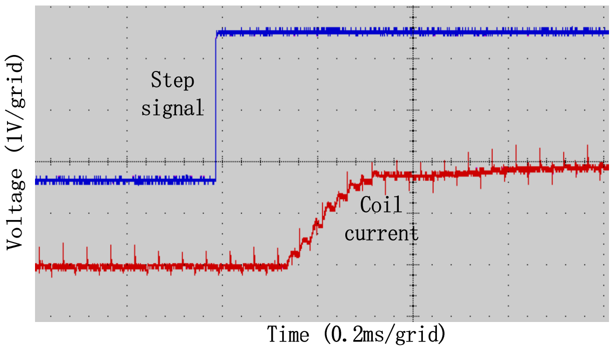

(3) The test result with Kp =32

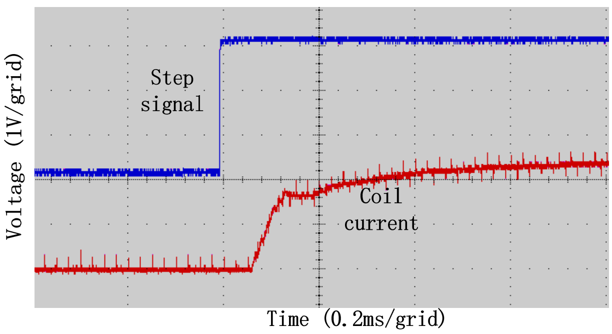

(4) the test result with Kp = 64

Fig.13 The comparison of simulation results and test results with different Kd

V. CONCLUSION

This paper analyzes detailed the working principle of three-level power amplifier, the simulation model of three-level power amplifier of AMB based on FPGA chip is built, which using MATLAB/Simulink Power System block and M-file. The simulation results are compared with the actual test results, it shows that the result of simulation models is accurate, the influence of different parameters on the amplifier dynamic characteristics are test with the simulation models. The results are shown that bus voltage had the greatest influence the dynamic characteristics of a power amplifier, proportional coefficient Kp is smaller, and the differential coefficient is smallest. So the method offers a new thought for analyzing the dynamic characteristics of the PA for AMB.

ACKNOWLEDGEMENTS

This research work was financially supported by Natural Science Foundation of China (11302120), Natural Science Foundation of Shandong Province (ZR2011EEQ029) and (ZR2012EEM031), and "National Natural Science Foundation of China" (51075236) and "The Fundamental Research Funds of Shandong University"（2015JC042）).

REFERENCES

[1] G Schweitzer, H Bleuler, A Traxler, Active Magnetic Bearings, ETH, 1994
[2] Wang Jiqiang, Wang Fengxiang, Kong Xiaoguang. Design and analysis of electromagnetic properties for high speed PM generator [J]. Proceedings of the CSEE, 28(20): 105-110,2008.
[3] Wang Jiqiang, Wang Fengxiang, Zong Ming. Critical speed calculation of magnetic bearing-rotor system for a high speed machine[J]. Proceedings of the CSEE, 27(27): 94-98,2007.
[4] Xu Yanliang, Fang Jiancheng. Development of low power loss energy storage flywheel[J]. Transactions of China Electrotechnical Society, 23(12): 11-16,2008.
[5] Fan Yahong, Fang Jiancheng, Experimental research on the mutational stability of magnetically suspended momentum wheel in control moment gyroscope [C], Proceedings of the ninth international symposium on magnetic bearings. Lexington, Kentucky, USA2004.
[6] Zhang Liang, Fang Jiancheng, Analysis of Current Ripple and Implementation of Pulse Width Modulation Switching Power Amplifiers for Active Magnetic Bearing[J], TRANSACTIONS OF CHINA ELECTROTECHNICAL SOCIETY, Vol.33, Mar, 13-20,2007.
[7] DONG Shu-cheng, FANG Jian-cheng, YU Wenbo, Study on Dynamic Stability of Flywheel Rotor Supported by AMB Based on PID Controller[J], ,Journal of Astronautics, 26(3): 296-300,2005.
[8] Zang Xiaomin, Wang Xiaolin, Qiu Zhijian, et al. An improved current-controlled tristate switching power amplifier for magnetic bearings based on sample-hold strategy [J]. Transactions of China Electrotechnical Society, 19(10): 85-90,2004.
[9] Zang Xiaomin, Wang Xiaolin, Qiu Zhijian, Research on current mode tri-state modulation technology in switching power amplifier for magnetic bearings[J]. Proceedings of the CSEE, 24(9): 167-172, 2004.
[10] HUANG Yong, XU Long-xiang, Simulation of Switching Power Amplifier for Active Magnetic Bearing Applications Based on MULTISIM[J], Machinery & Electronics,4, 10-13, 2009.
[11] Zhang Liang, Fang Jiancheng. Research on modeling and simulation of switching power amplifier for active magnetic bearing applications based on MATLAB[J]. Journal of System Simulation, 19(11): 2395-2398,2007.
[12] Wang Jun, Xu Long xiang, System Modeling and Control for Switching Power Amplifier of Magnetic Bearings, China Mechanical Engineering[J], 4, 477-481,2010.